Supplementary Material (ESI) for Journal of Materials Chemistry

SUPPORTING INFORMATION

Water-soluble magnetic glyconanoparticles based on metal-doped ferrites coated with gold: synthesis and characterization

Juan Gallo, Isabel García, Daniel Padro, Blanca Arnáiz, and Soledad Penadés

Laboratory of GlycoNanotechnology, Biofunctional Nanomaterials Unit, CIC biomaGUNE/CIBER-BBN, Pº de Miramón 182, 20009 San Sebastian, Spain

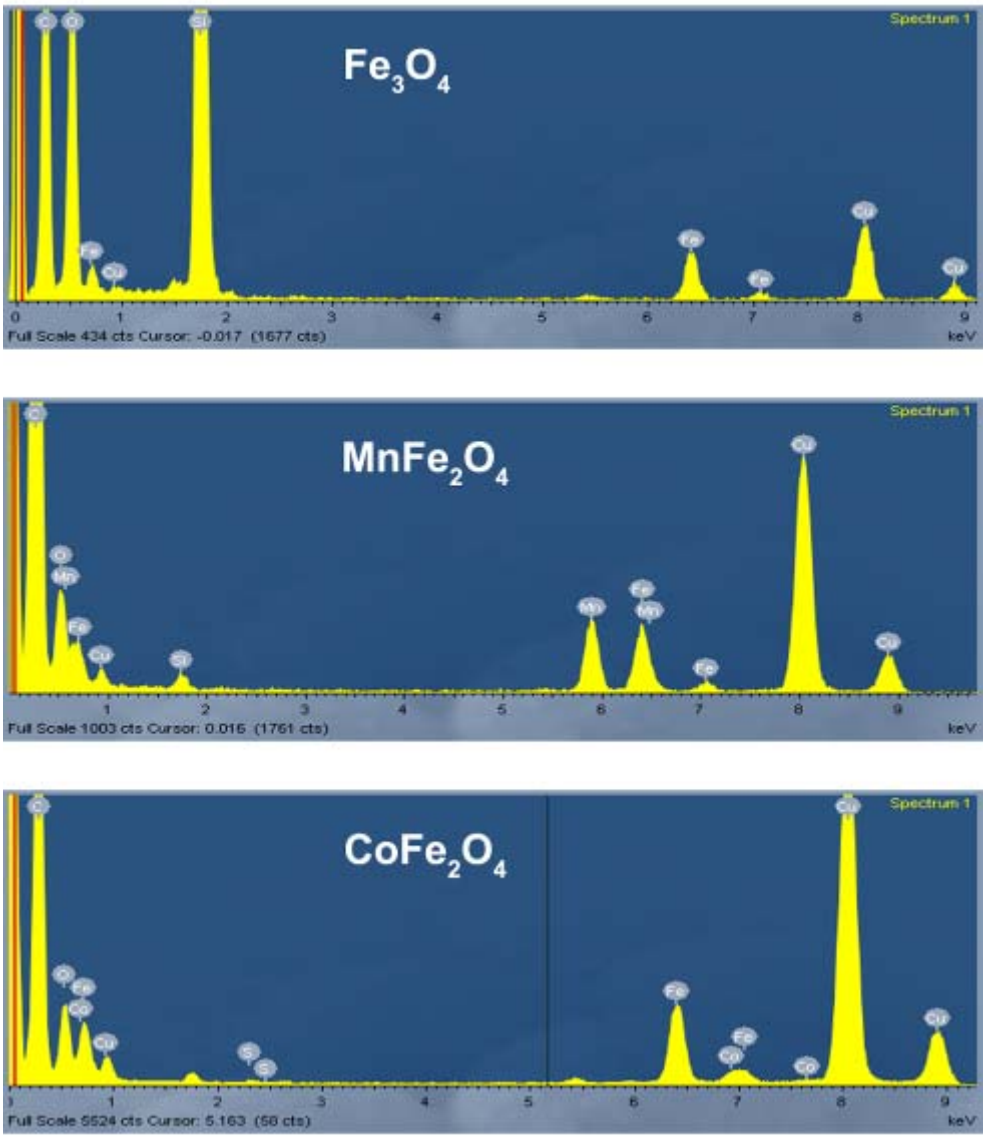

S1. EDX spectra of Fe_3O_4 (upper), $MnFe_2O_4$ (centre) and $CoFe_2O_4$ (lower). Peaks from Cr (around 5.5 KeV) and Si (around 1.7 KeV) are present in the three spectra coming from the sample holder.

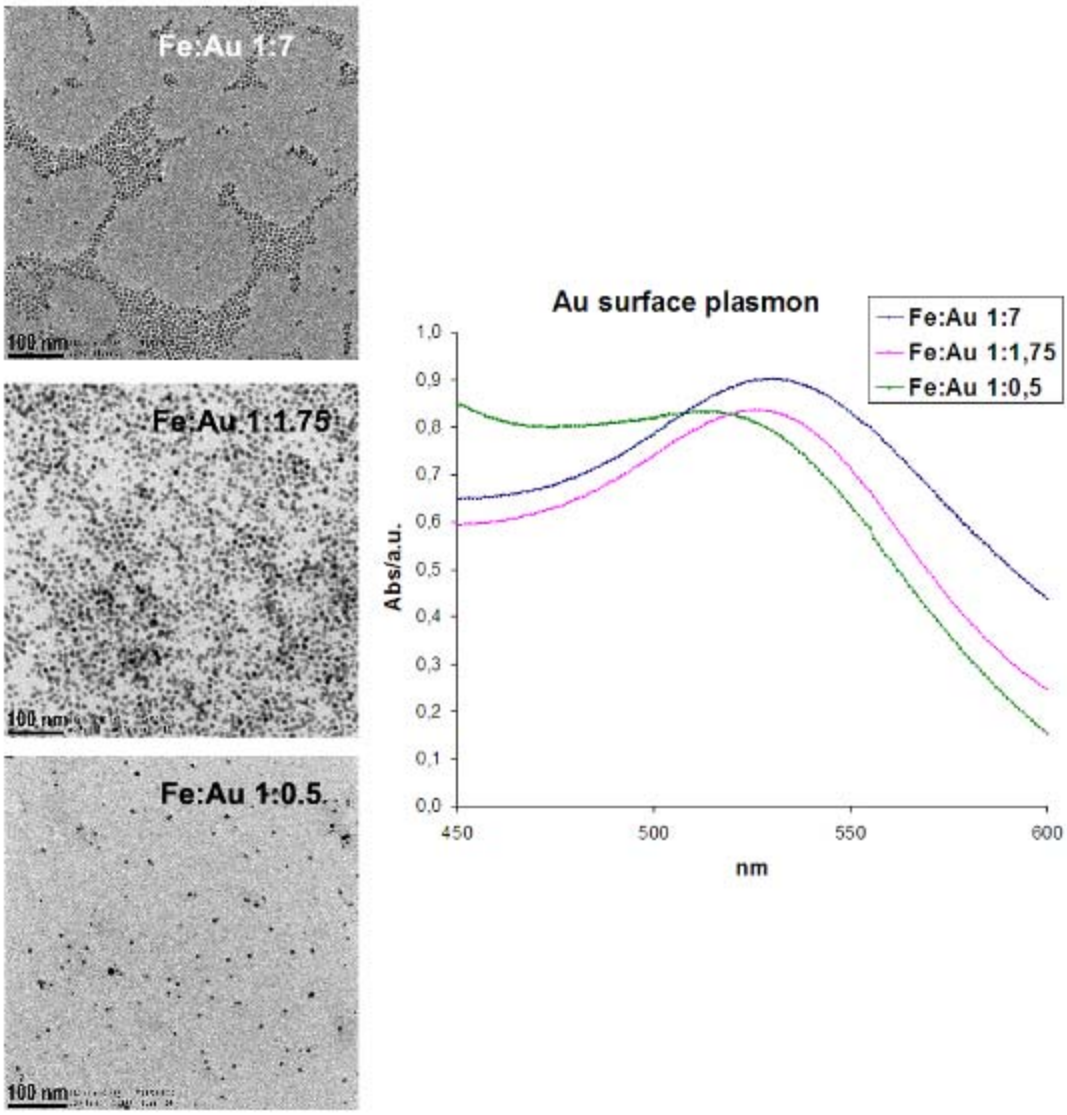

S2. Left: TEM micrograph of the Fe_3O_4@Au nanoparticles obtained from the coating reactions at different Fe/Au ratio. Right: UV-Vis spectra of the same nanoparticles showing a red shift in the position of the Au surface plasmon resonant peak.

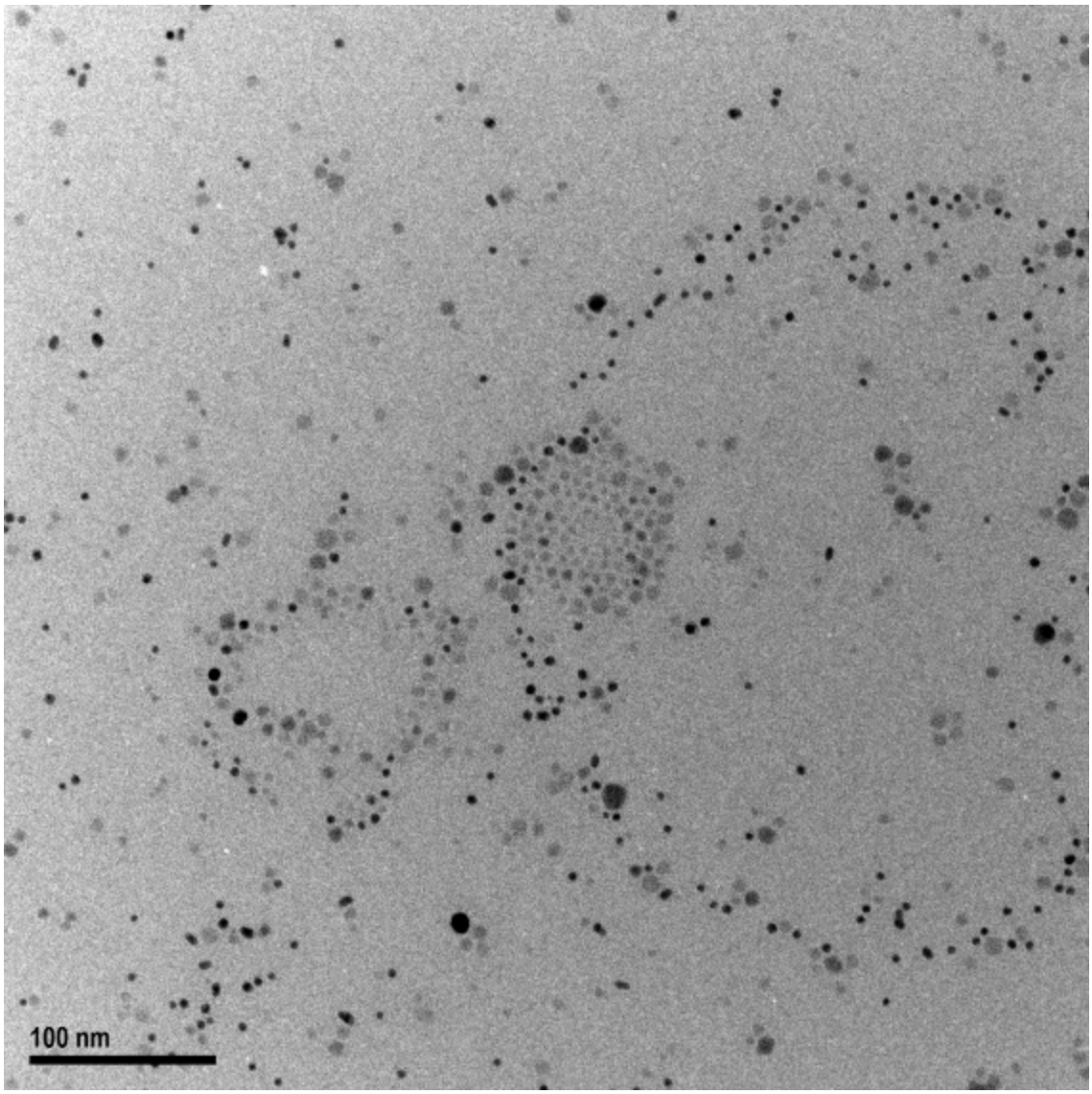

S3. TEM micrograph of nanoparticles obtained under Zhong's conditions for the coating of $MnFe_2O_4$ nanoparticles.

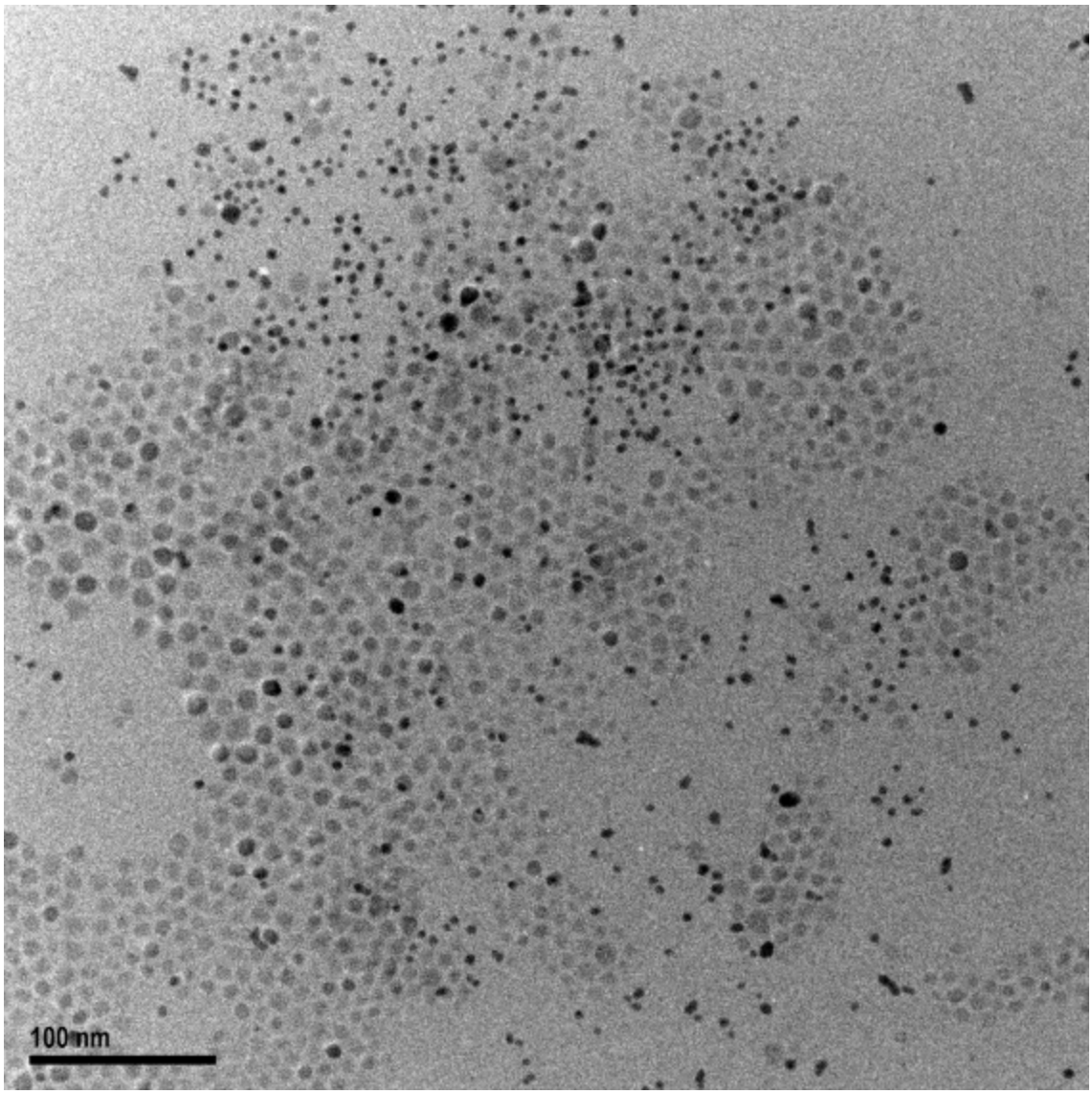

S4. TEM micrograph of a failed gold coating reaction of $MnFe_2O_4$ nanoparticles, after purification by magnetic sorting out and centrifugation.

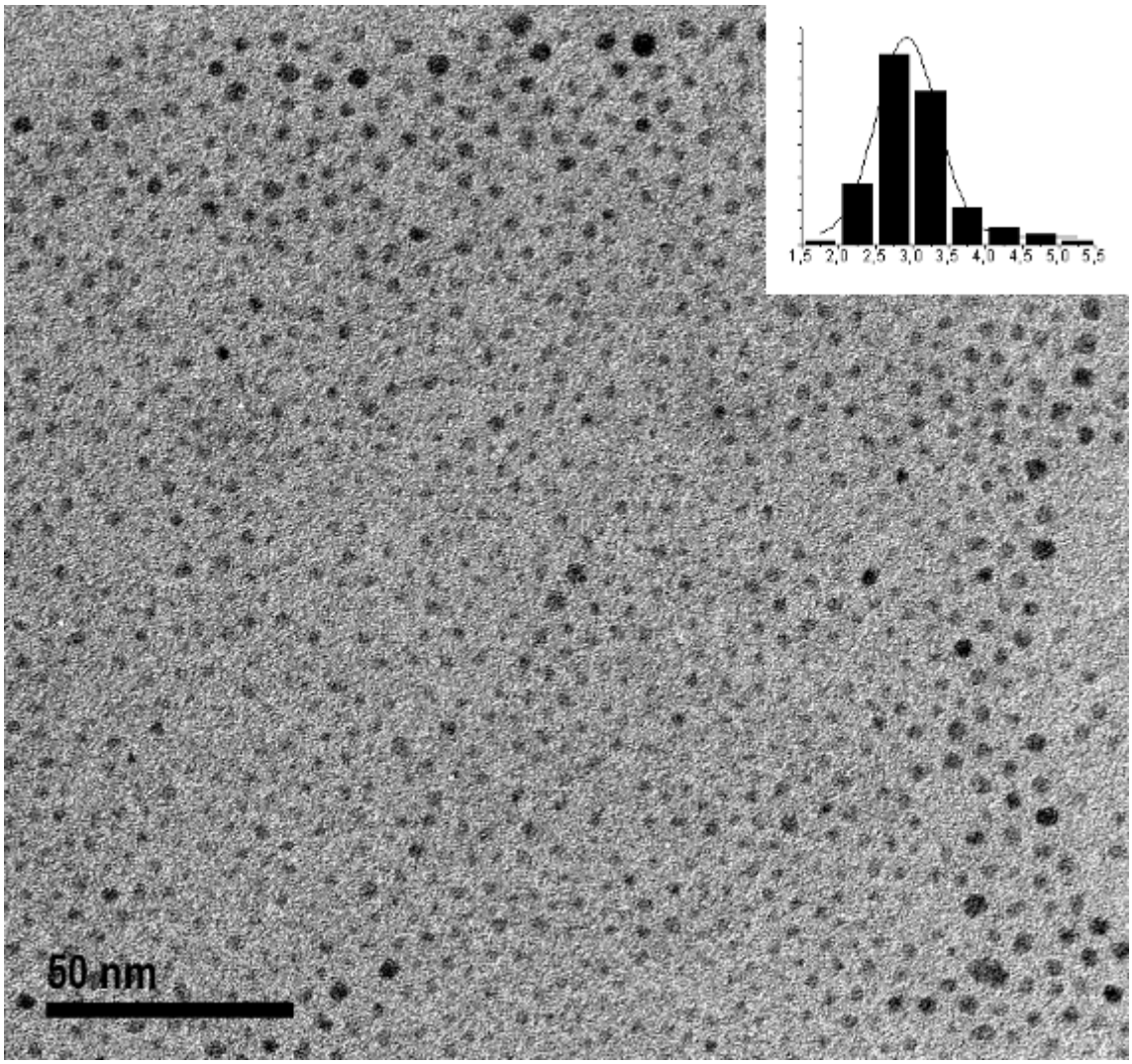

S5. TEM micrograph of 3.2 nm Fe_3O_4 nanoparticles. Insert, size distribution diagram of the sample.

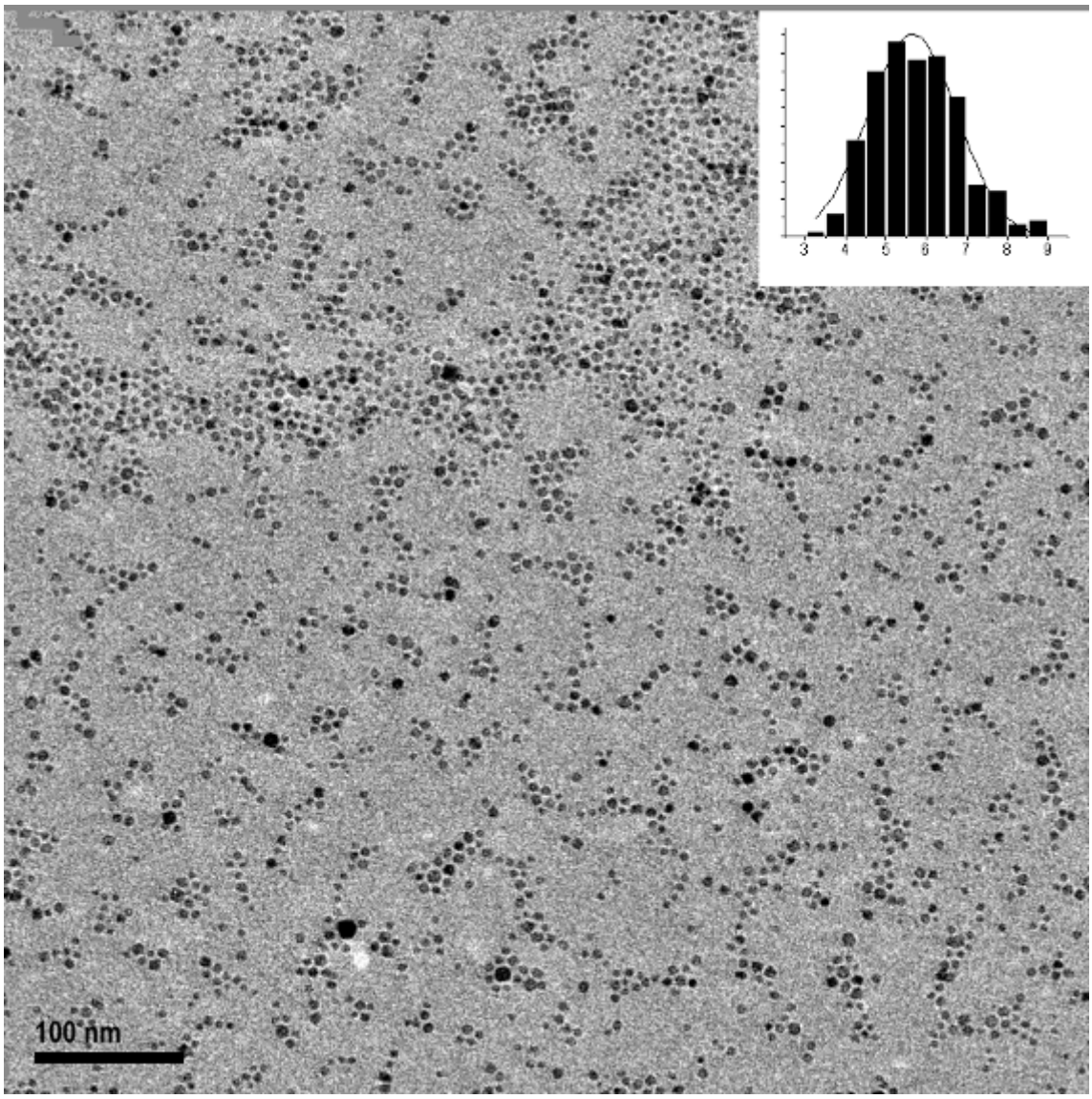

S6. TEM micrograph of 6.1 nm $MnFe_2O_4$ nanoparticles. Insert, size distribution diagram of the sample.

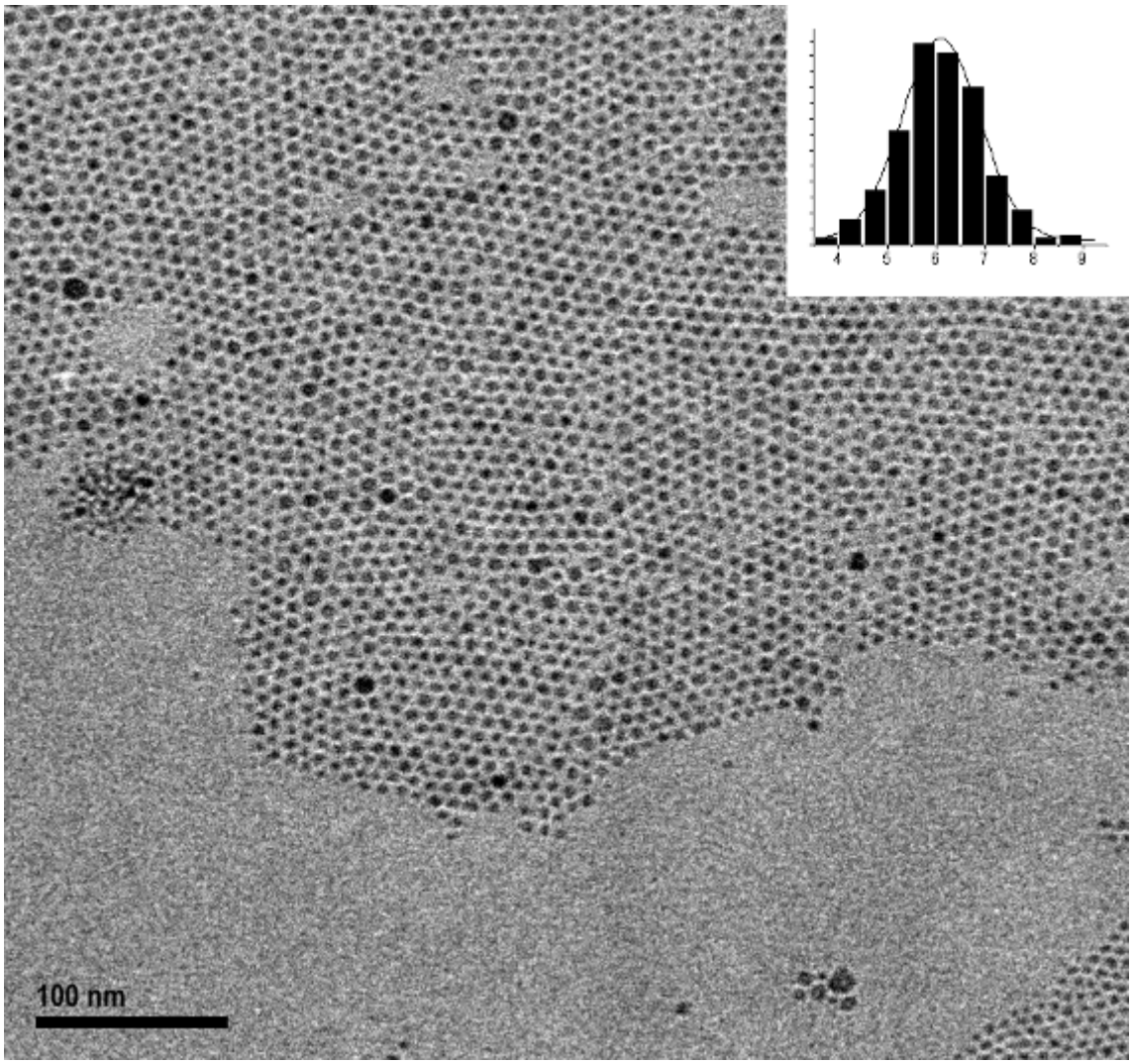

S7. TEM micrograph of 6.2 nm $CoFe_2O_4$ nanoparticles. Insert, size distribution diagram of the sample.

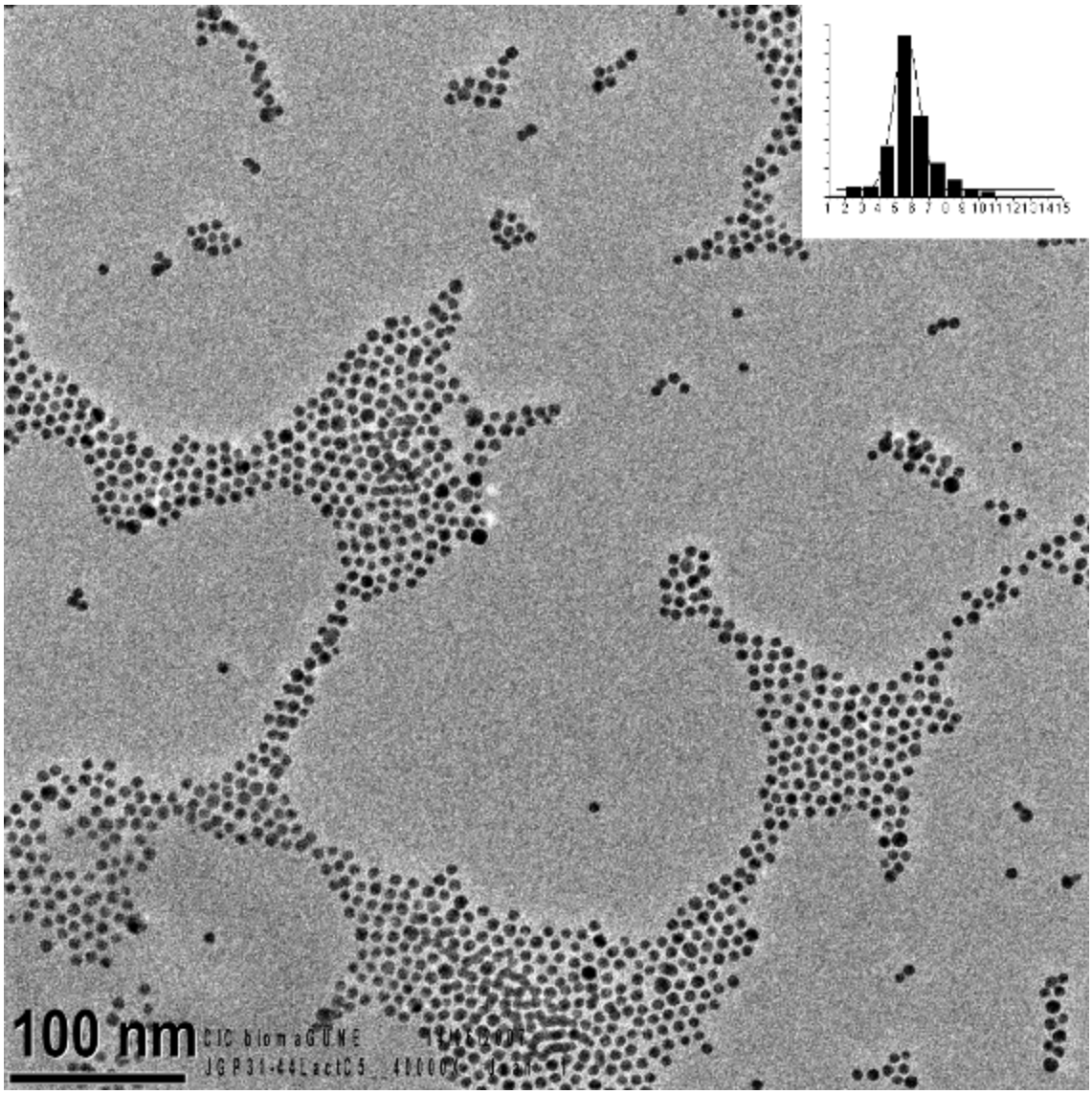

S8. TEM micrograph of 5.4 nm Fe_3O_4@Au nanoparticles. Insert, size distribution diagram of the sample.

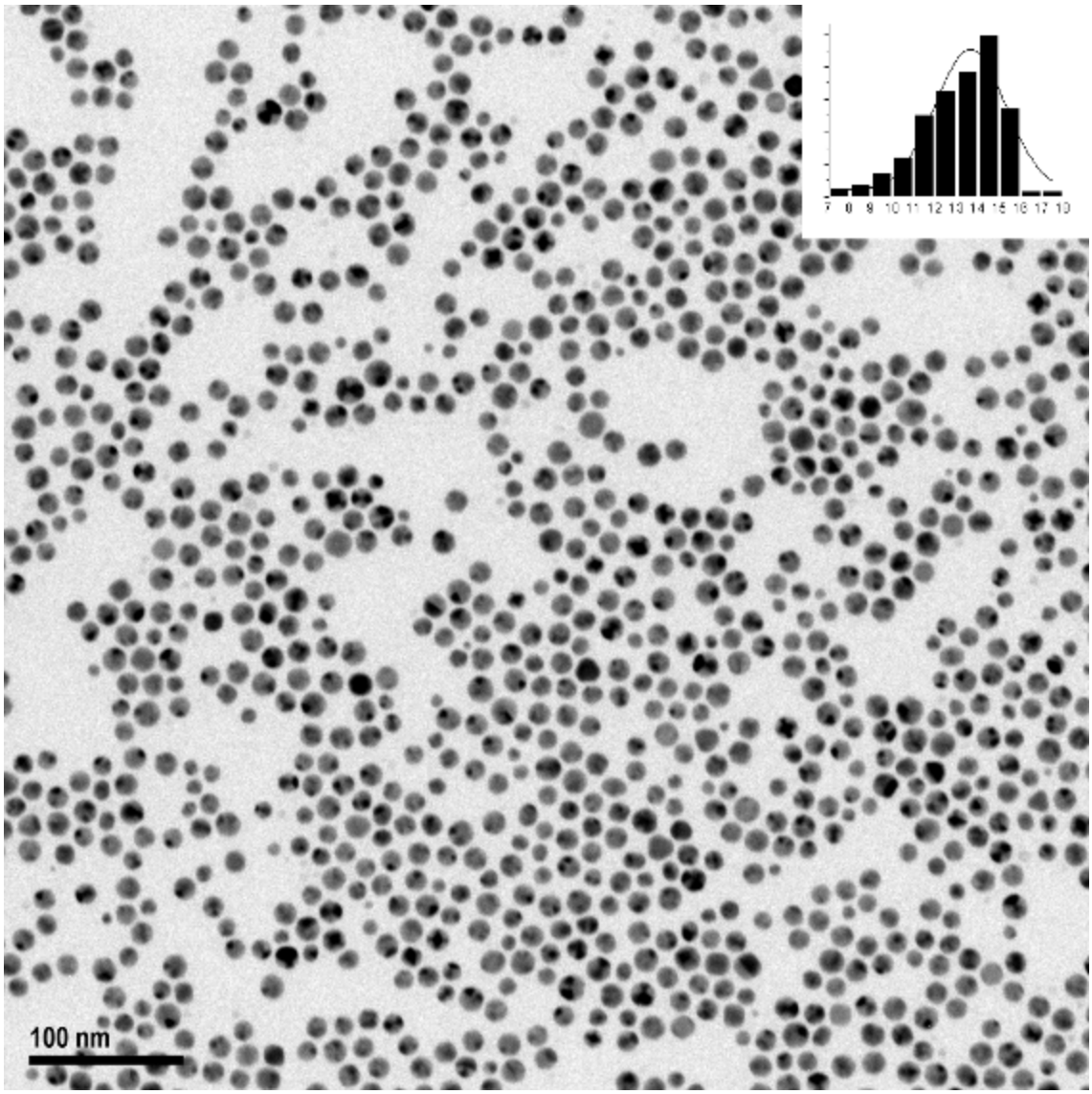

S9. TEM micrograph of 13.5 nm $MnFe_2O_4$@Au nanoparticles. Insert, size distribution diagram of the sample.

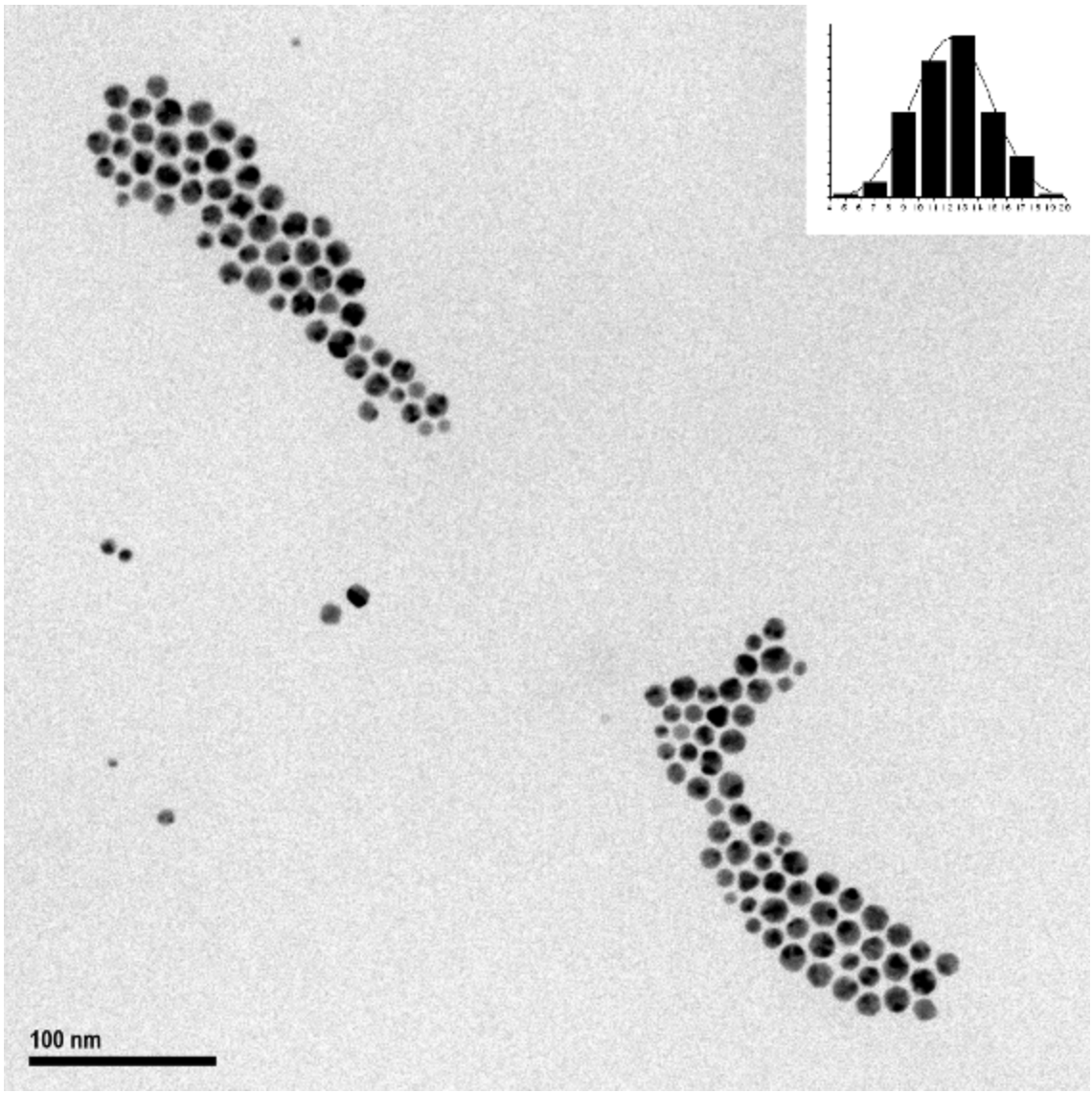

S10. TEM micrograph of 12.5 nm $CoFe_2O_4$@Au nanoparticles. Insert, size distribution diagram of the sample.

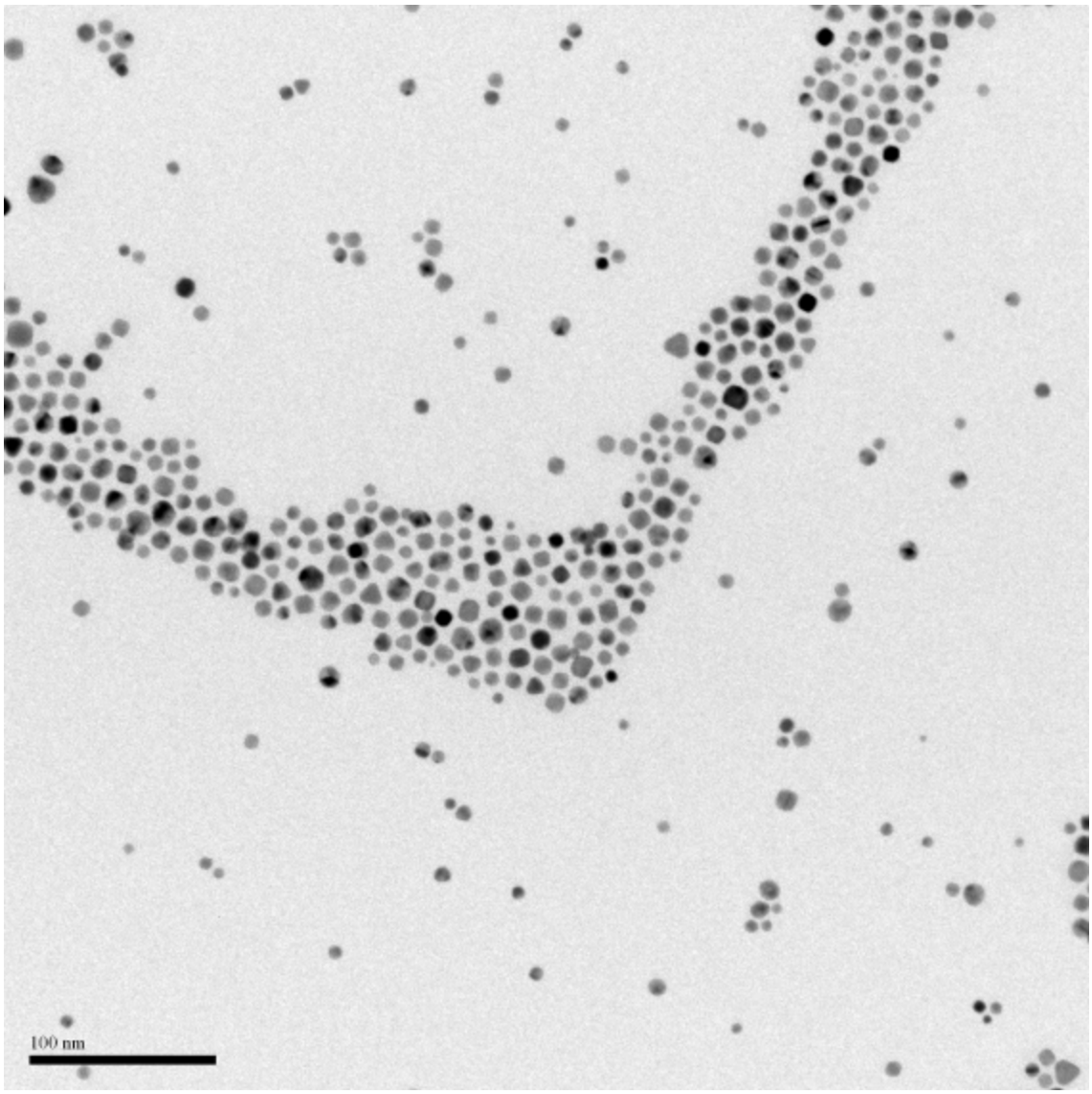

S11. TEM micrograph of Au nanoparticles obtained from the coating reaction of $MnFe_2O_4$ without the magnetic seeds.

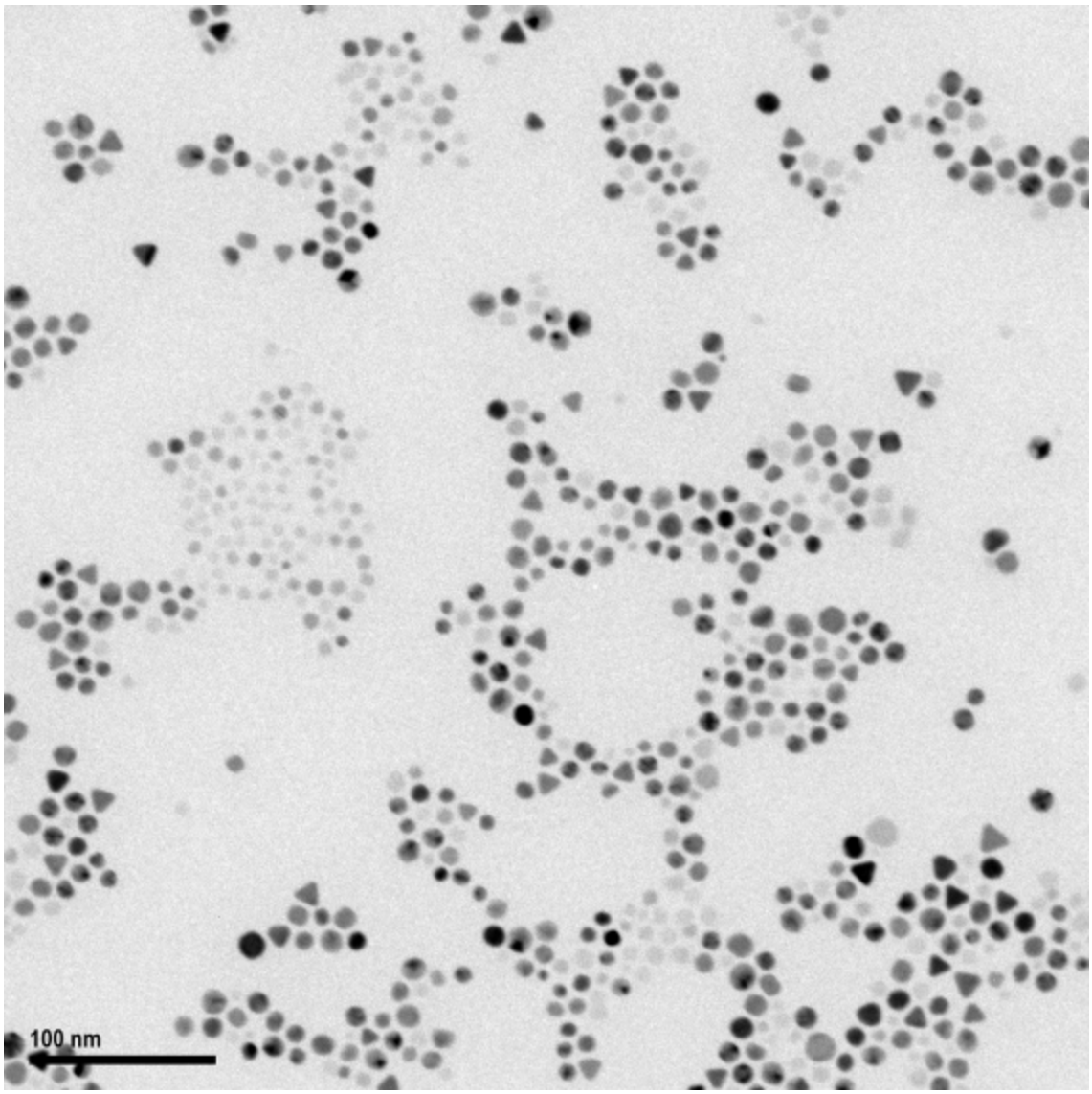

S12. TEM micrograph of nanoparticles obtained from the coating reaction of $MnFe_2O_4$ with insufficient Au reagent.

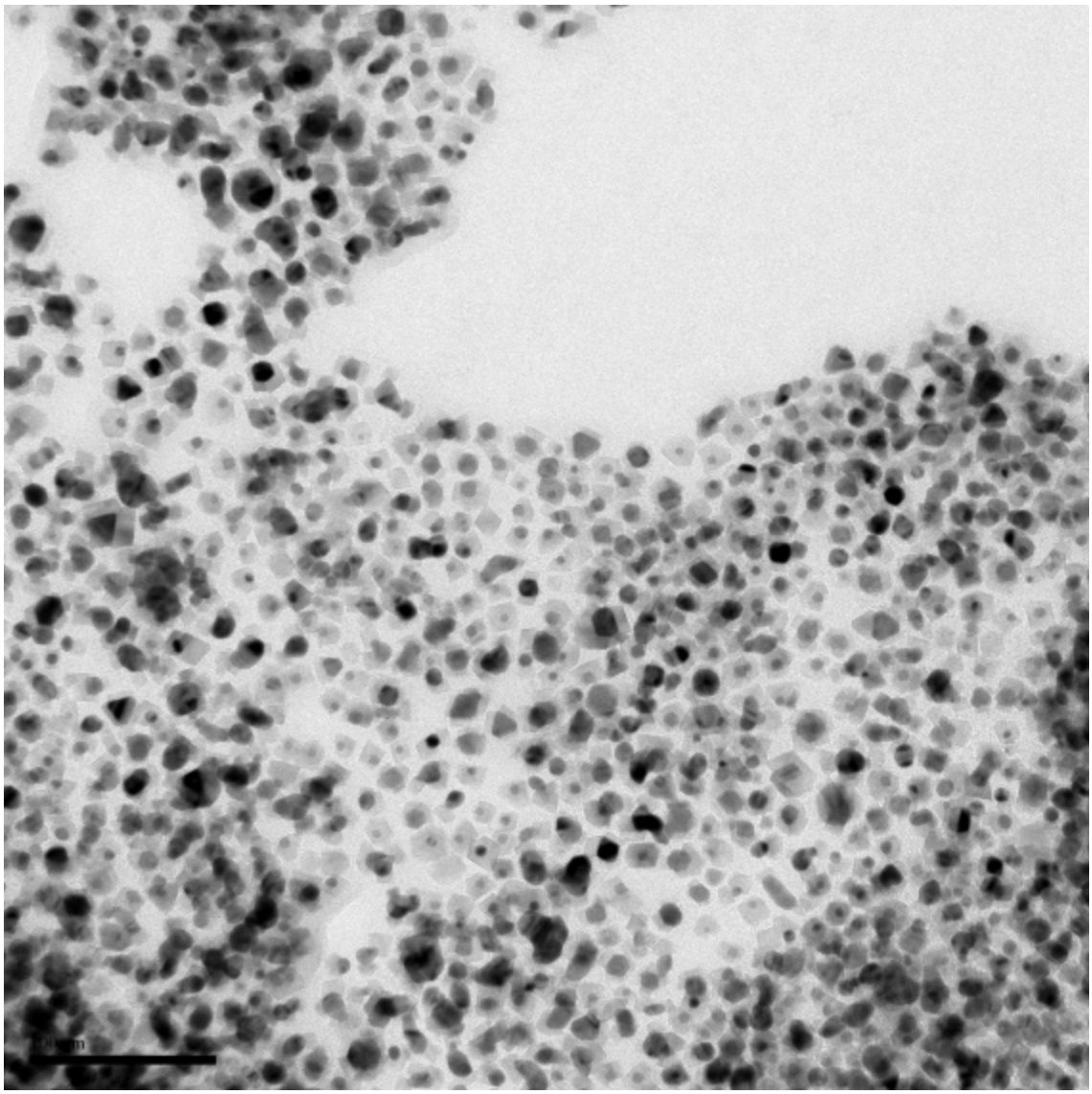

S13. TEM micrograph of Au@$MnFe_2O_4$ structures obtained when the synthesis of the Mn ferrite cores was performed in the presence of Au reagent.

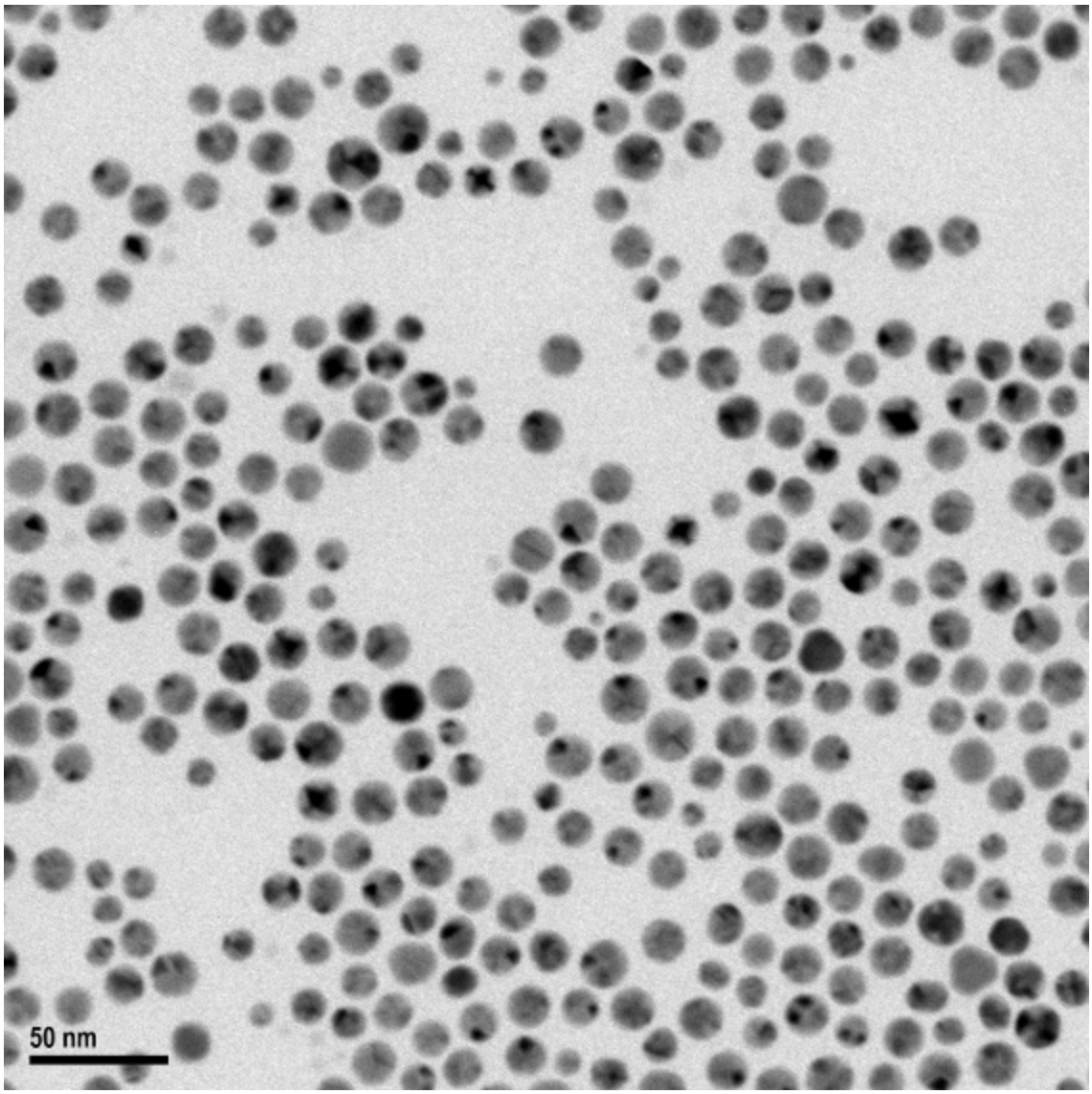

S14. TEM micrograph of $MnFe_2O_4$@Au nanoparticles obtained under the modified gold coating conditions.

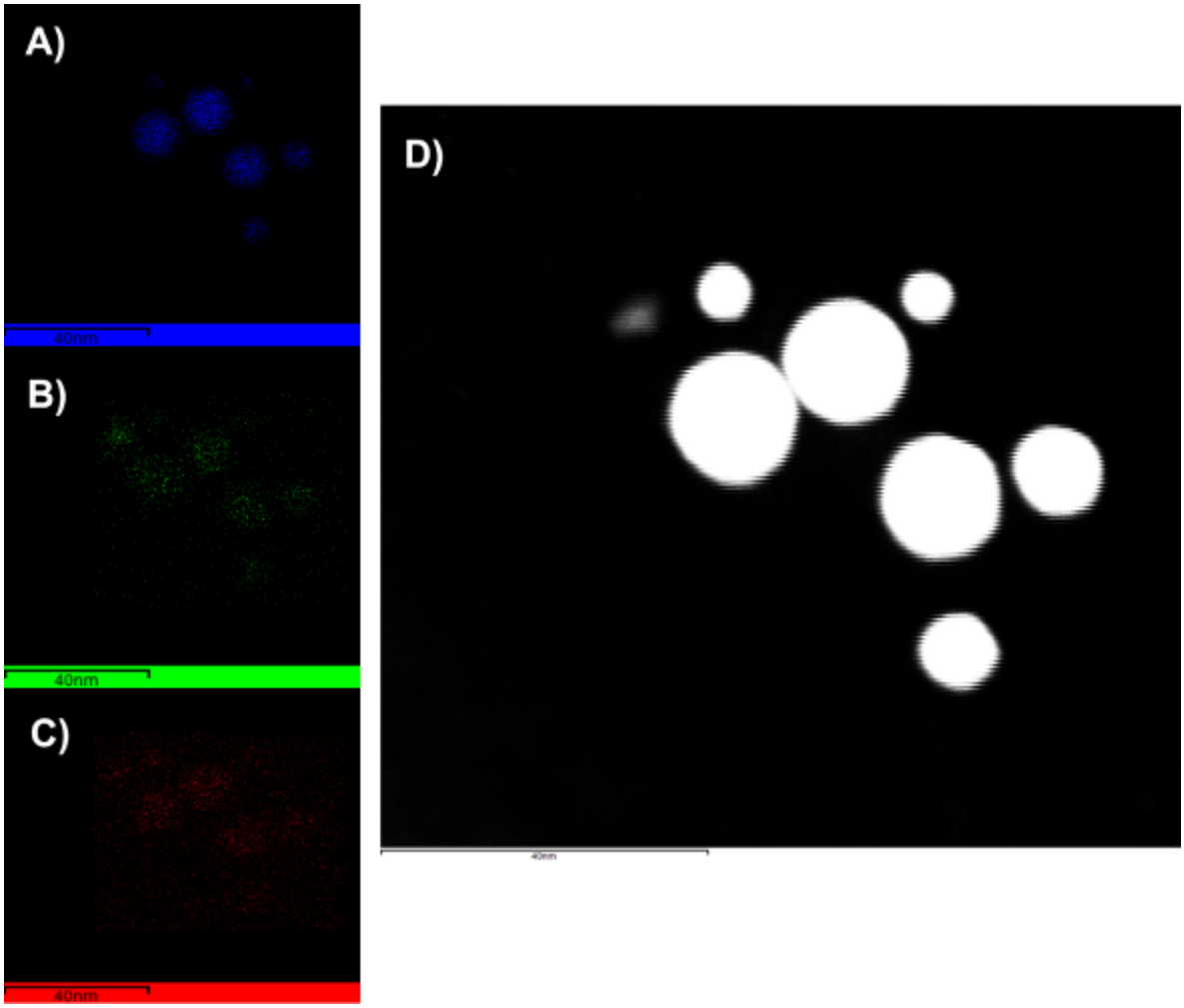

S15. STEM-EDXS elemental mapping of $MnFe_2O_4$@Au nanoparticles. **A**) Au map, **B**) Fe map, **C**) O map, **D**) STEM image.

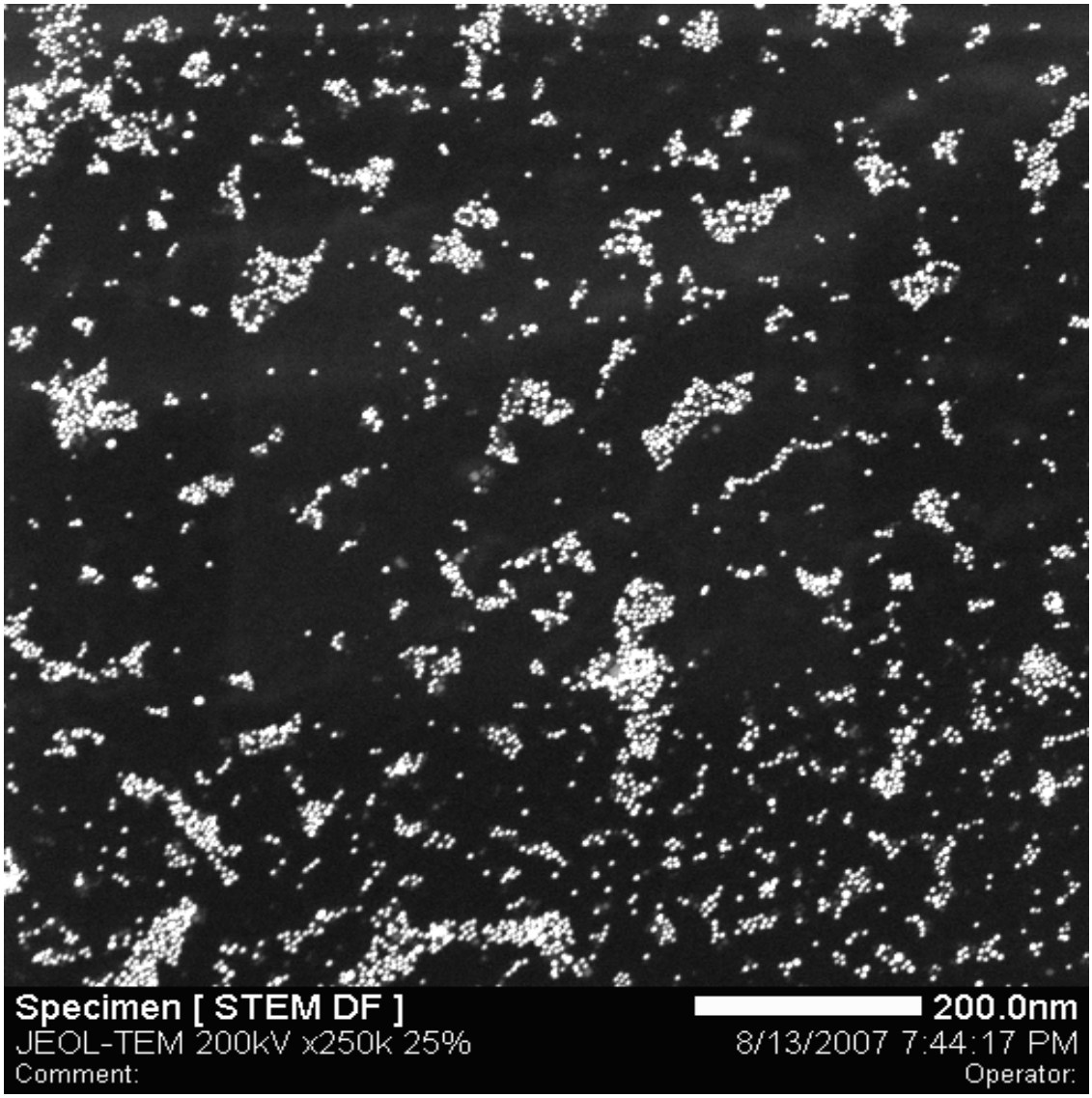

S16. STEM micrograph of Fe_3O_4@Au nanoparticles

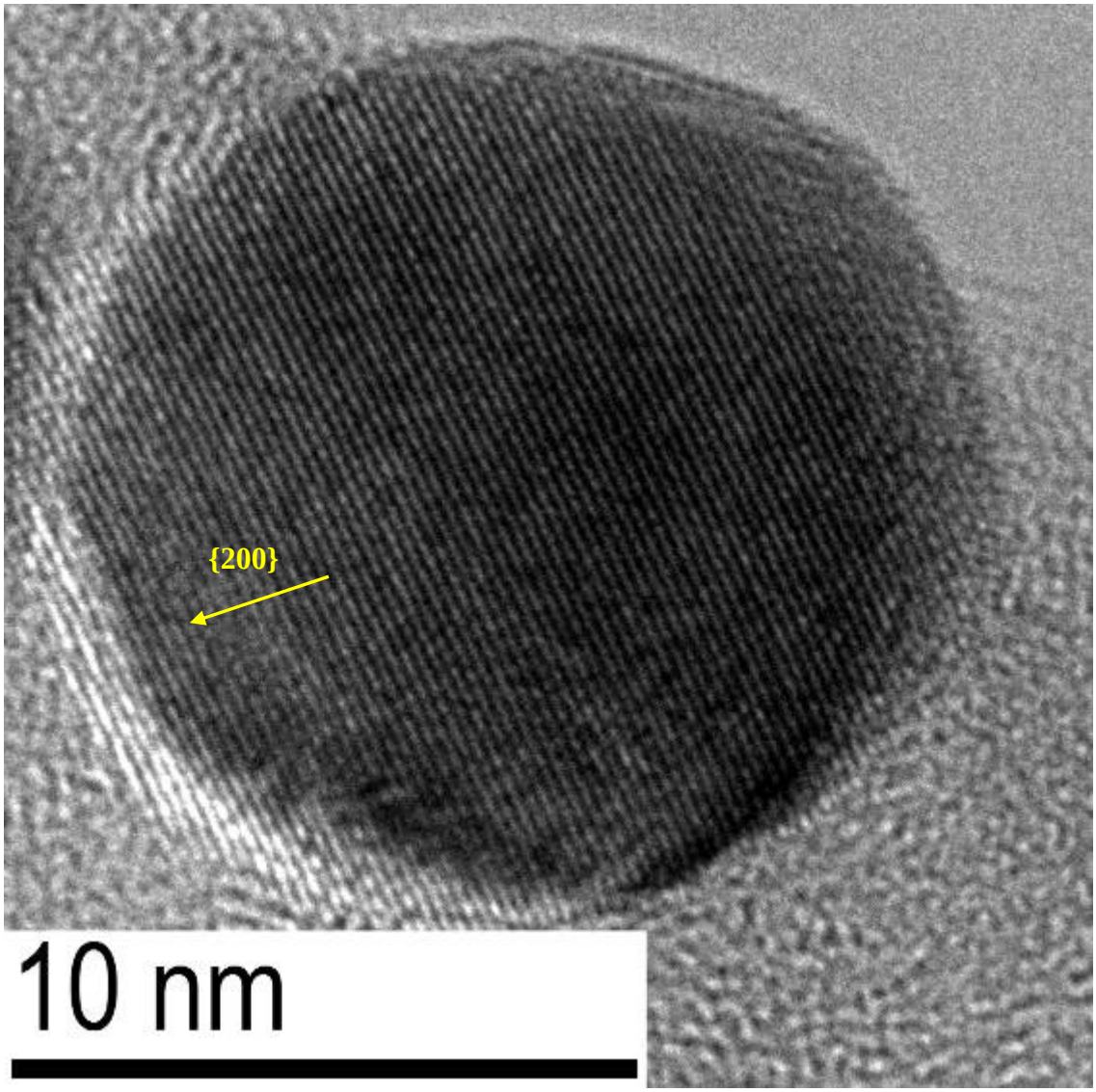

S17. HR TEM micrograph of $MnFe_2O_4$@Au nanoparticles. Lattice spacing is clearly visible and the spacing between fringes can be measured to be ~ 2.04 Å, in agreement with {200} lattice planes of face-centred cubic (fcc) Au.

ICP-OES analysis	Fe	Mn	Co	Au
Fe_3O_4@Au@LactC_{11}/Linker	25.2 %	0 %	0 %	74.8 %
$MnFe_2O_4$@Au@LactC_{11}/Linker	6.04 %	2.54 %	0 %	91.42 %
$CoFe_2O_4$@Au@LactC_{11}/Linker	6.72 %	0 %	2.87 %	90.43 %

S18. ICP-OES analysis of the metal content of the three different *glyco*-ferrites. Previous to the ICP-OES analysis samples were solved in aqua regia.

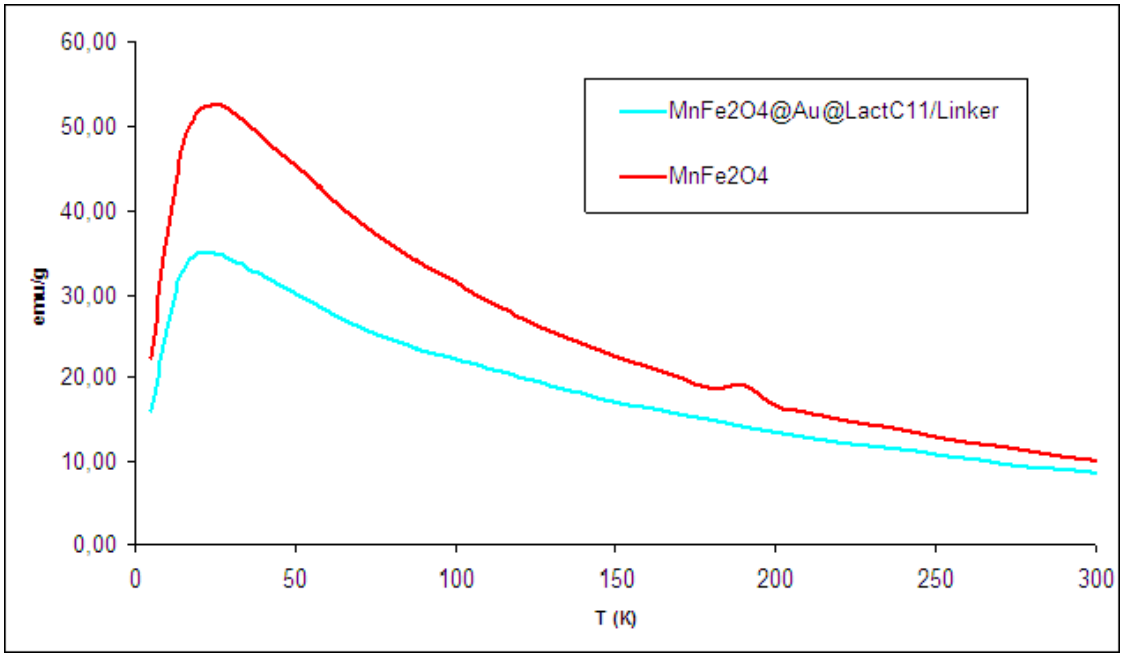

S19. Comparison of blocking temperature for $MnFe_2O_4$ (red) and $MnFe_2O_4$@Au@LactC_{11}/Linker (blue) at H = 100 Oe

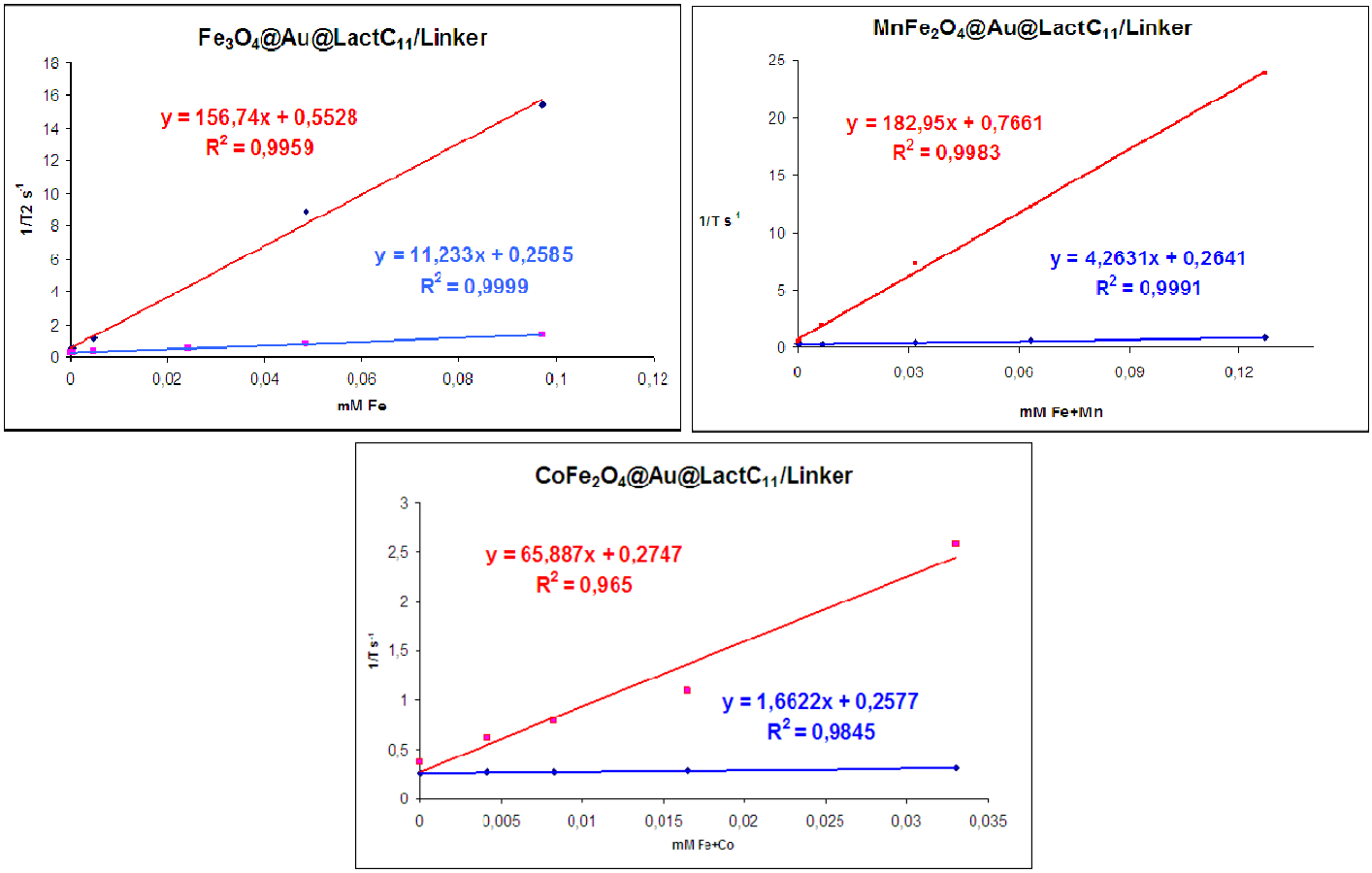

S20. Plots of the relaxivity rates *vs* the concentration of magnetic material to calculate the relaxivity values r_1 (blue) and r_2 (red) from the slope of the linear fit of the data. Plots of Fe_3O_4@Au@LactC_{11}/Linker (upper-left), $MnFe_2O_4$@Au@LactC_{11}/Linker (upper-right), and $CoFe_2O_4$@Au@LactC_{11}/Linker (bottom).

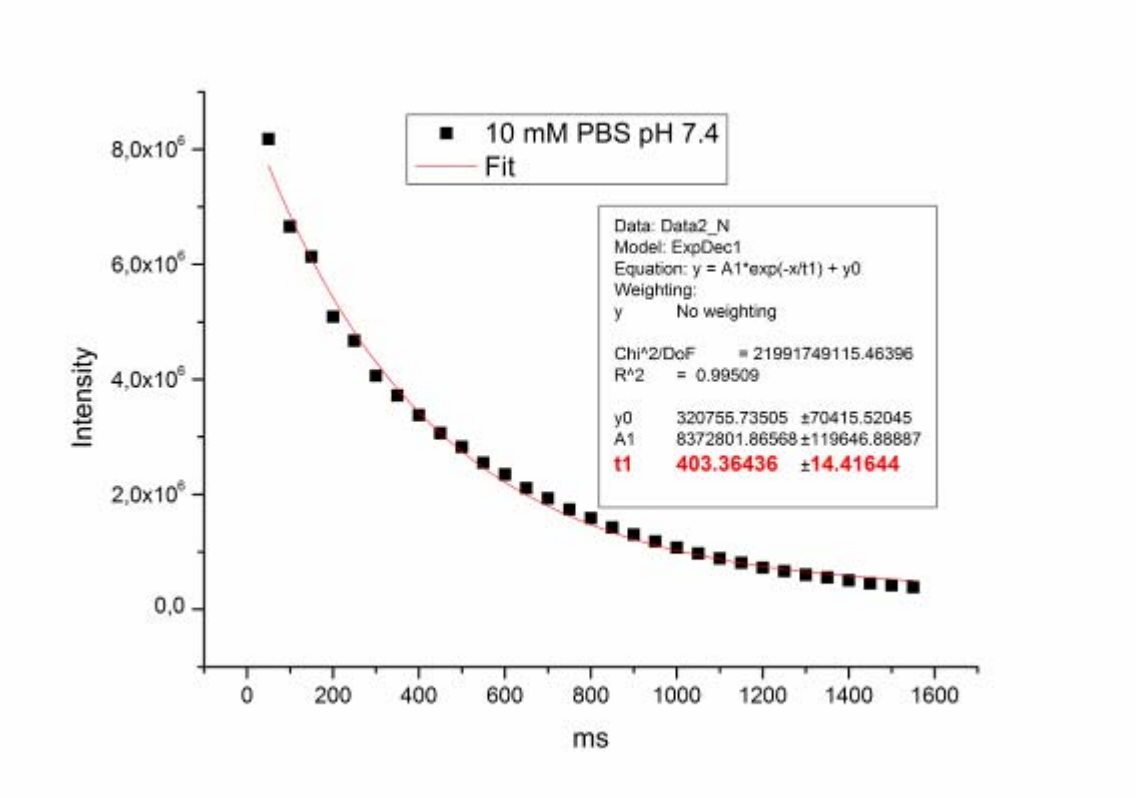

S21. T2 measurement of 10 mM PBS pH 7.4 obtained from MRI phantoms at 11.7 T.

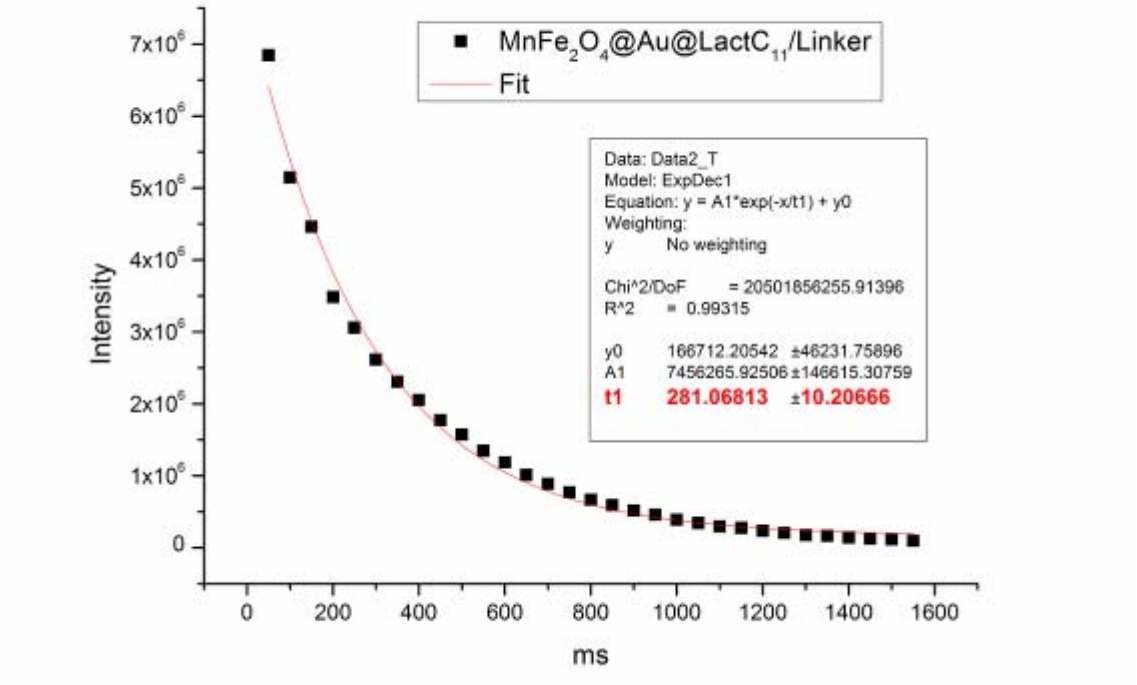

S22. T2 measurement of $MnFe_2O_4$@Au@$LactC_{11}$/Linker at a concentration of 62.5 μM of magnetic material, obtained from MRI phantoms at 11.7 T.

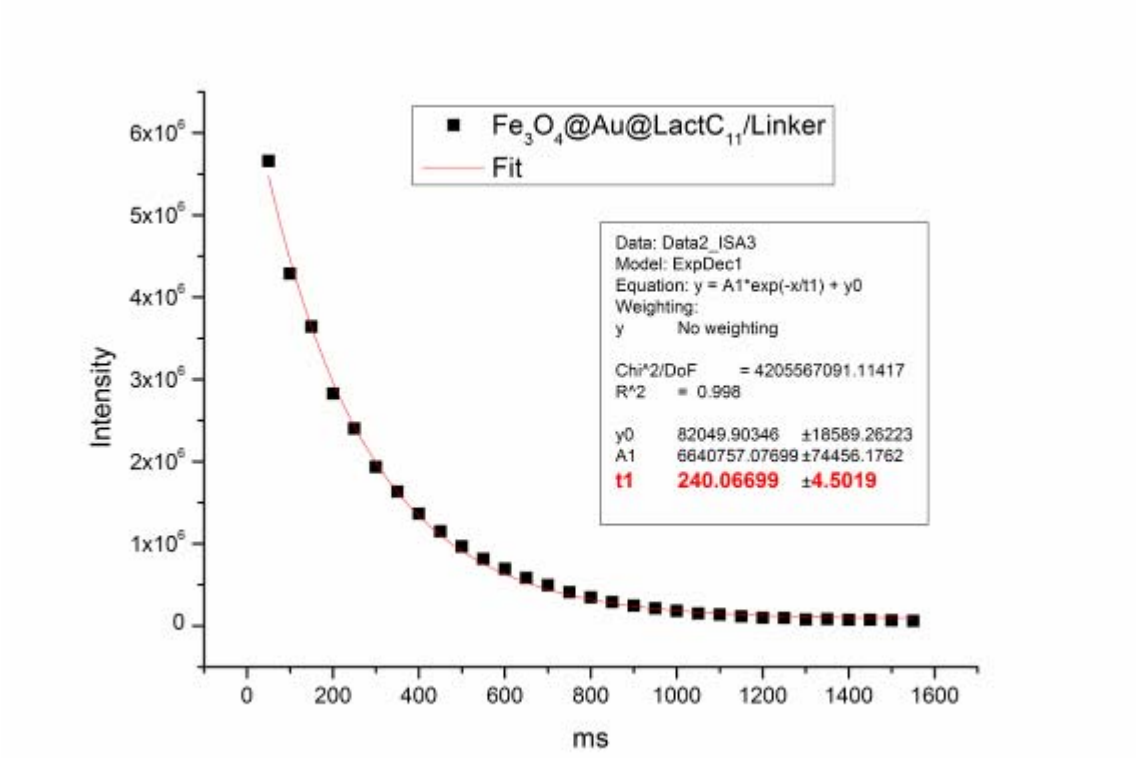

S23. T2 measurement of Fe_3O_4@Au@$LactC_{11}$/Linker at a concentration of 62.5 μM of magnetic material, obtained from MRI phantoms at 11.7 T.

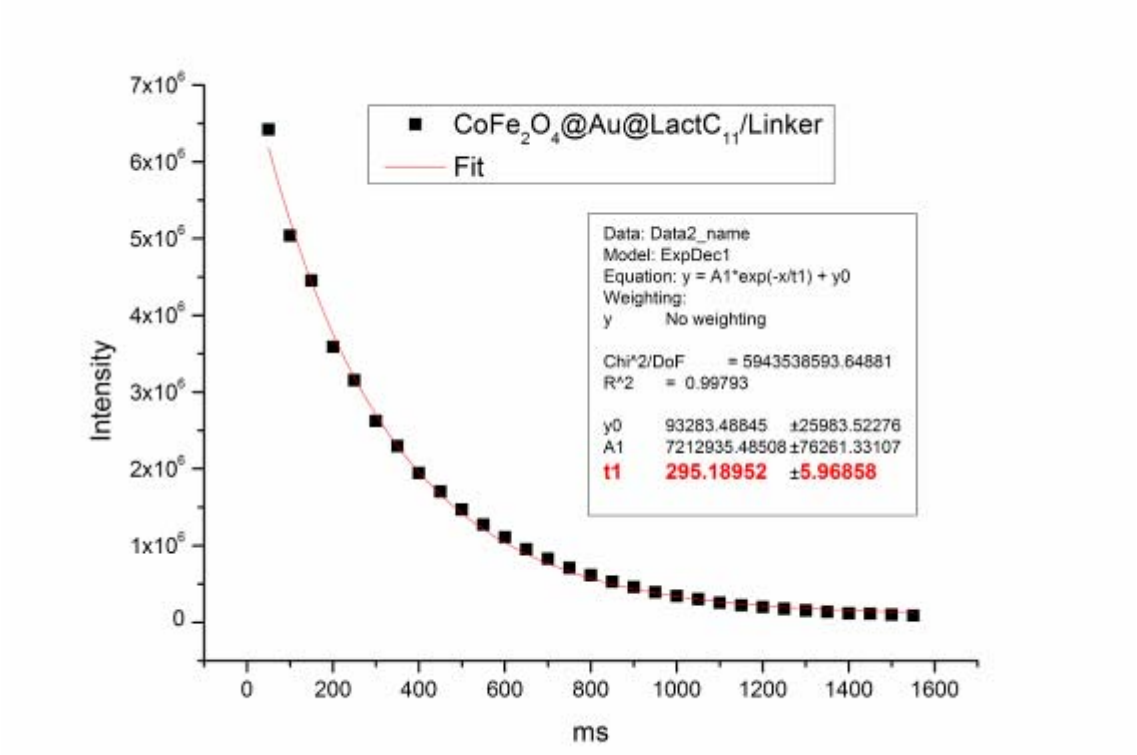

S24. T2 measurement of $CoFe_2O_4$@Au@$LactC_{11}$/Linker at a concentration of 62.5 μM of magnetic material, obtained from MRI phantoms at 11.7 T.

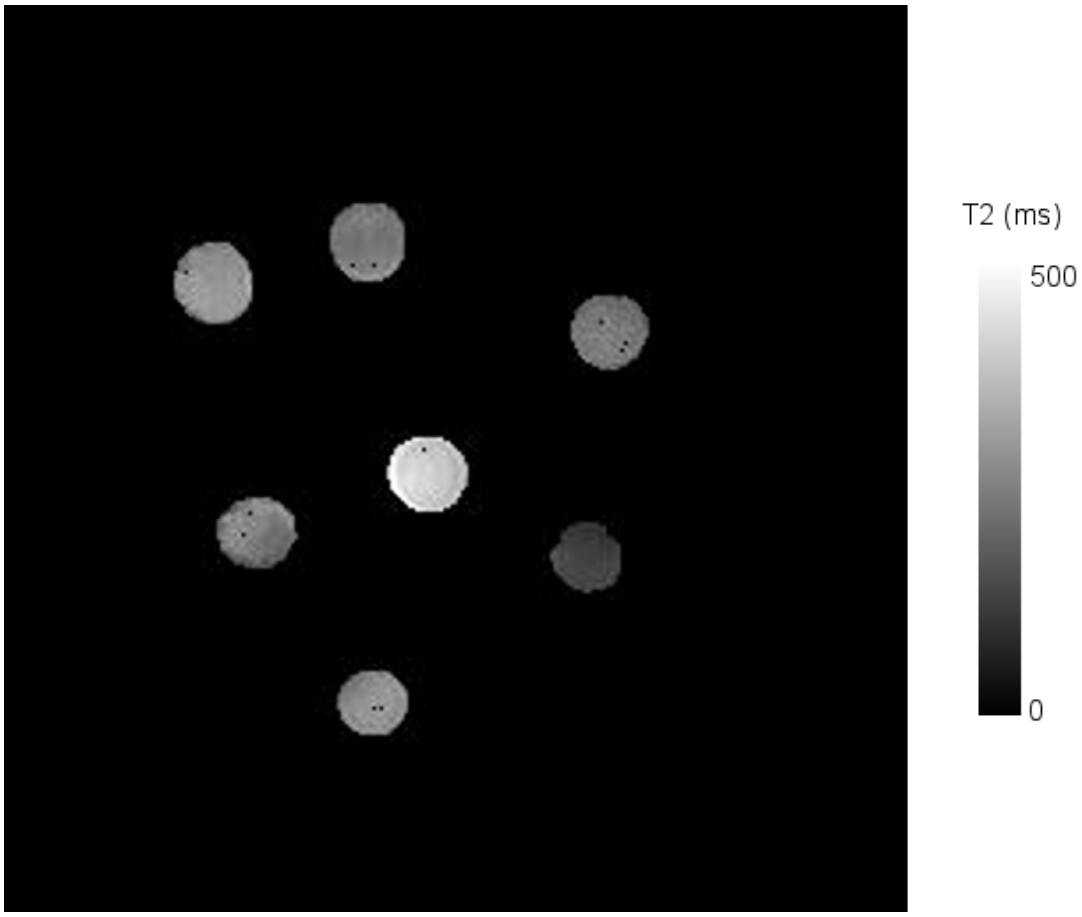

S25. T_2-weighed MRI image of the different phantoms measured at 11.7 T.

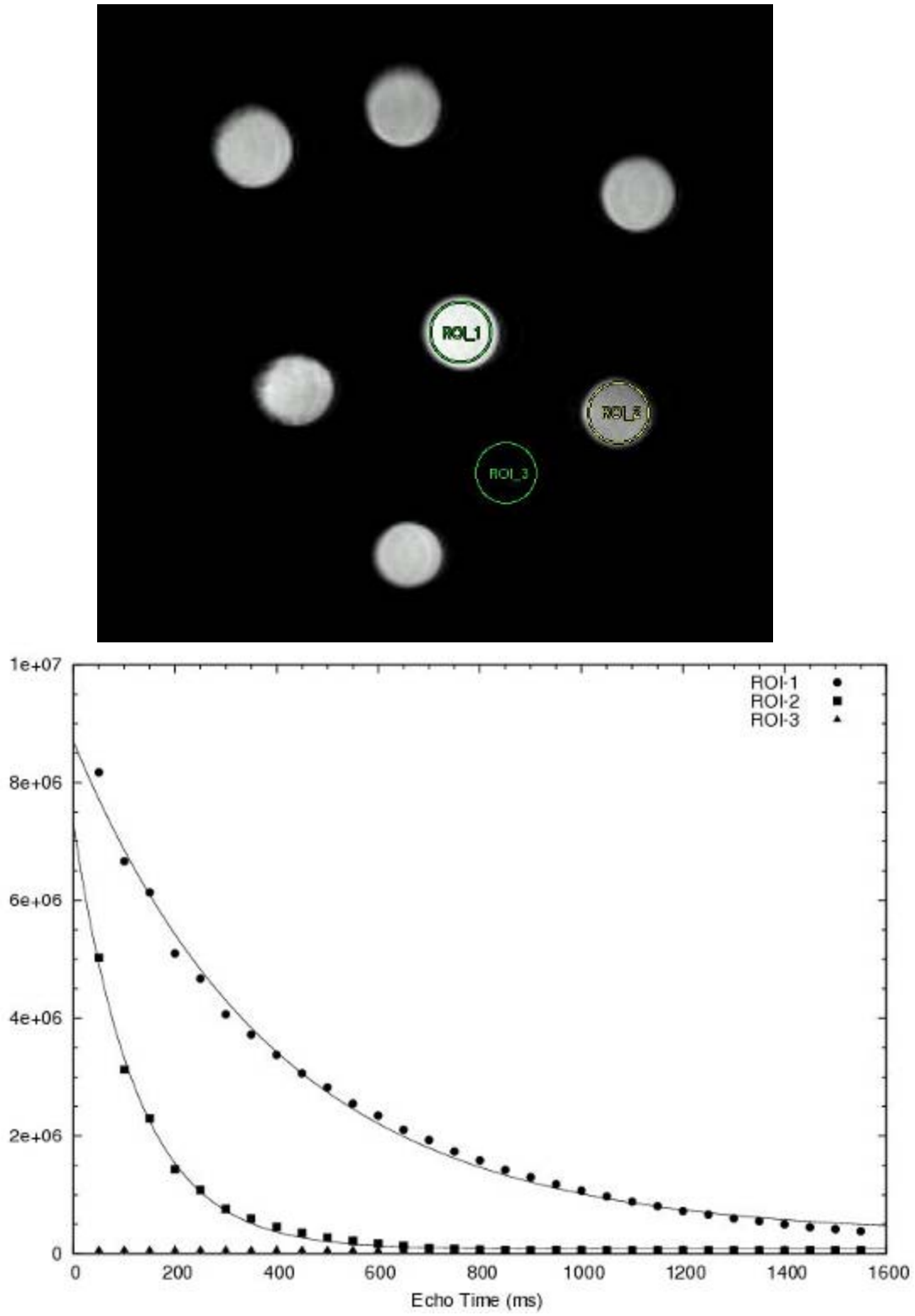

S26. Up, regions of interest (ROI) in the phantoms with the longest T_2 (ROI_1), the shortest T_2 (ROI_2), and the background (ROI_3). Down, T_2 plots of the three ROIs to demonstrate the difference between the signal and the noise (background).